

X-ray Detector XRD on BeEagleSat and the Development of the Improved X-ray Detector iXRD

Dr. Emrah Kalemci
*Faculty of Engineering and Natural
Sciences Sabancı University*
Istanbul, Turkey
ekalemci@sabanciuniv.edu

Dr. Ayhan Bozkurt
*Faculty of Engineering and Natural
Sciences Sabancı University*
Istanbul, Turkey
abozkurt@sabanciuniv.edu

Kaan Veziroğlu
*Faculty of Engineering and Natural
Sciences Sabancı University*
Istanbul, Turkey
kveziroglu@sabanciuniv.edu

M. Erdem Baş
*Gumush Space Istanbul,
Turkey*
erdembas17@gmail.com

M. Deniz Aksulu
*Anton Pannekoek Institute of
Astronomy University of Amsterdam*
Amsterdam, the Netherlands
M.D.Aksulu@uva.nl

M. Ertan Ümit
*Instrumentation and Electronic
Laboratory The von Karman Institute
for Fluid Dynamics Sint-Genesius-Rode,
Belgium*
m.e.umit@vki.ac.be

Dr. A. Rüstem Aslan
*Faculty of Aeronautics and
Astronautics Istanbul Technical
University*
Istanbul, Turkey
aslanr@itu.edu.tr

Milad Diba
*Faculty of Engineering and Natural
Sciences Sabancı University*
Istanbul, Turkey
mdiba@sabanciuniv.edu

M. Şevket Uludağ
*Faculty of Aerospace Engineering
Delft University of Technology*
Delft, the Netherlands
m.s.uludag@tudelft.nl

Abstract—Many interesting astrophysical objects are intense X-ray emitters. Hard X-ray observatories in various sizes have been operating in space and providing exciting scientific results that we cannot obtain in our laboratories on Earth. Nanosatellites with CdZnTe hard X-ray detectors have been launched into orbit as well, and the future holds great promise with such small satellites contributing significantly to high energy astrophysics. One of those satellites is the BeEagleSat which carried the X-ray detector (XRD) to low Earth orbit. The XRD has a $15 \times 15 \times 3$ mm³ volume CdZnTe detector, a cross-strip electrode design, a RENA readout chip controlled by an MSP 430 microcontroller. Due to a communication problem with the receiver, no science data could have been downloaded from the XRD.

Recently, an improved version of the XRD has been designed (called the iXRD) and currently it is in the production phase. The improvements compared to the XRD are the larger volume crystal with almost three times the collecting area, a collimator to limit the field of view for focused scientific return, and a motherboard-daughterboard design to reduce electronic noise.

Keywords—Space technology; payloads, Sensors; X-ray detectors

The iXRD detector development is supported by TUBITAK Project no 116F151

I. INTRODUCTION

X-rays are produced under extreme conditions (strong gravity, large magnetic fields) in the universe and some of the most interesting astrophysical objects such as neutron star and black hole X-ray binaries, gamma-ray bursts, and magnetar bursts can be extremely bright [1]. Since the atmosphere is opaque to X-rays, detectors are placed in satellites and observations are conducted in different orbits around the Earth. The X-ray observatories in space can have different types of detectors and telescopes, and their sizes and complexity vary immensely. While many of the scientific work has been done with large observatories, small observatories with a focus on specific sources and processes contribute significantly to high energy astrophysics as well. There is no lower limit in size, nanosats with astrophysical payloads have been operating in space and will continue to deliver scientific results by filling key gaps that large observatories cannot touch [2].

At Sabancı University High Energy Astrophysics Detector Laboratory (HEALAB) we design and produce X-ray detector systems utilizing CdZnTe material. CdZnTe hard X-ray de-

tectors operate between 20 keV – 300 keV, and have been used in previous missions [3], [4]. To qualify our detector systems in space we developed and delivered the "X-ray detector (XRD)" which is currently in orbit on BeEagleSat. The placement of XRD on BeEagleSat is shown in Fig. 1 left panel. BeEagleSat is one of the 2U cubesats of the European Commission Framework 7 QB50 network (<https://www.qb50.eu/index.html>). BeEagleSat was released from the ISS on May 26, 2017 (see Fig. 1, right panel). The details of the operation and the status of the XRD are discussed in Section II.

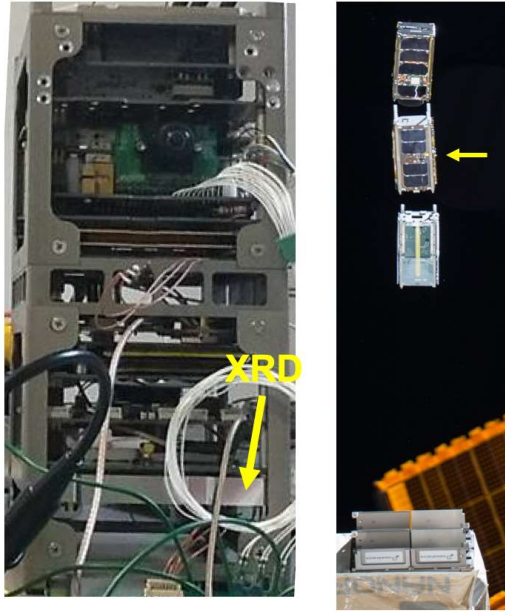


Fig. 1. Left: BeEagleSat during pre-flight testing. Placement of XRD is shown with the yellow arrow. The detector is enclosed in aluminum to protect from stray light and electrons. Right: BeEagleSat (shown with yellow arrow) released from the ISS.

Apart from space qualification, the XRD was aimed at measuring the hard X-ray background in low Earth orbit as well as catching occasional gamma-ray bursts. There have been other nanosatellite missions utilizing CdZnTe detectors in hard X-rays. An earlier mission, AAUSAT II, included a single channel $10 \times 10 \times 3 \text{ mm}^3$ crystal with the aim of detecting gamma-ray bursts (<https://directory.eoportal.org/web/eoportal/satellite-missions/a/aausat-2>). Due to repeated rebooting of the on-board computer no science data could have been downloaded from the X-ray detector on AAUSAT-II. The other nanosatellites having CdZnTe detectors on-board are CXBN-I [5] and CXBN-II [6] of Morehead State University. Both satellites have the aim of increasing the precision of the Cosmic X-ray Background (CXRB) in 30 keV to 50 keV range. CXBN-I is a 2U cubesat and its' detector has 16×32 grid with $600 \times 600 \mu\text{m}$ pixels and two on-board calibration sources with a custom made read-out integrated circuit directly bonded to the detector pixels [5]. A graded-Z lead collimator restricts

the field of view to 36 degrees. CXBN-II, on the other hand, uses two commercial off-the-shelf (COTS) complete detector and readout electronics systems and a tungsten collimator prepared using additive manufacturing. The volume of each of the CXBN-II detectors is $40 \times 40 \times 6 \text{ mm}^3$.

II. XRD

The XRD (see Fig. 2) currently on BeEagleSat consisted of an orthogonal strip CdZnTe crystal, an application specific integrated circuit (RENA-3b ASIC) for readout, control electronics with an MSP 430 microcontroller, electrical power system including a high voltage (HV) power supply and associated coupling circuits. The evolution of the design and the development of the XRD can be found in [7] and [8]. The XRD was designed at HEALAB and developed in collaboration with Istanbul Technical University-Space Systems Design and Test Laboratory (ITU-SSDTL). Here, we describe the final design and properties of the XRD currently in low Earth orbit.

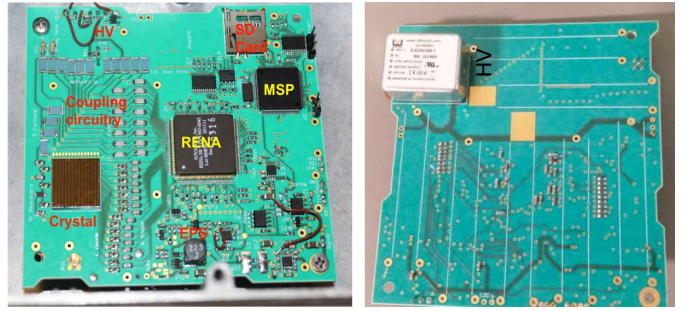


Fig. 2. Left: TOP layer of the XRD carrying the crystal and all of the active electronic components. Right: BOTTOM layer and the HV power supply.

A. The Detector and Readout Electronics

We used a CdZnTe crystal prepared at Due2Lab in Parma, Italy. This is a single crystal with good spectroscopic properties grown with the boron oxide vertical Bridgman technique. Details of the crystal growth and spectral properties can be found in [9].

The crystal has been cut to dimensions of $15 \times 15 \text{ mm}$ with a thickness of 2.5 mm. It is polished and chemically treated for surface passivation. Gold strips are deposited on both sides of the detector orthogonally with a pitch of 1 mm. The side that faces the PCB has 15 anode strips that are 0.25 mm wide and kept at ground potential. There are 3 sets of steering electrodes (also 0.25 mm wide) between the anode strips. They are kept at a lower potential (10% of the cathodes) to steer electrons towards the anodes, and their presence also enhances energy resolution due to small pixel effect [10], [11]. The electrode and steering electrode widths are optimized using extensive charge transport and collection simulations and experiments at HEALAB. On the opposite side, there are 15 orthogonal cathode strips that are 0.8 mm wide and are kept at -250 V. The cathode signals and high voltage are transmitted using gold wires from the crystal to

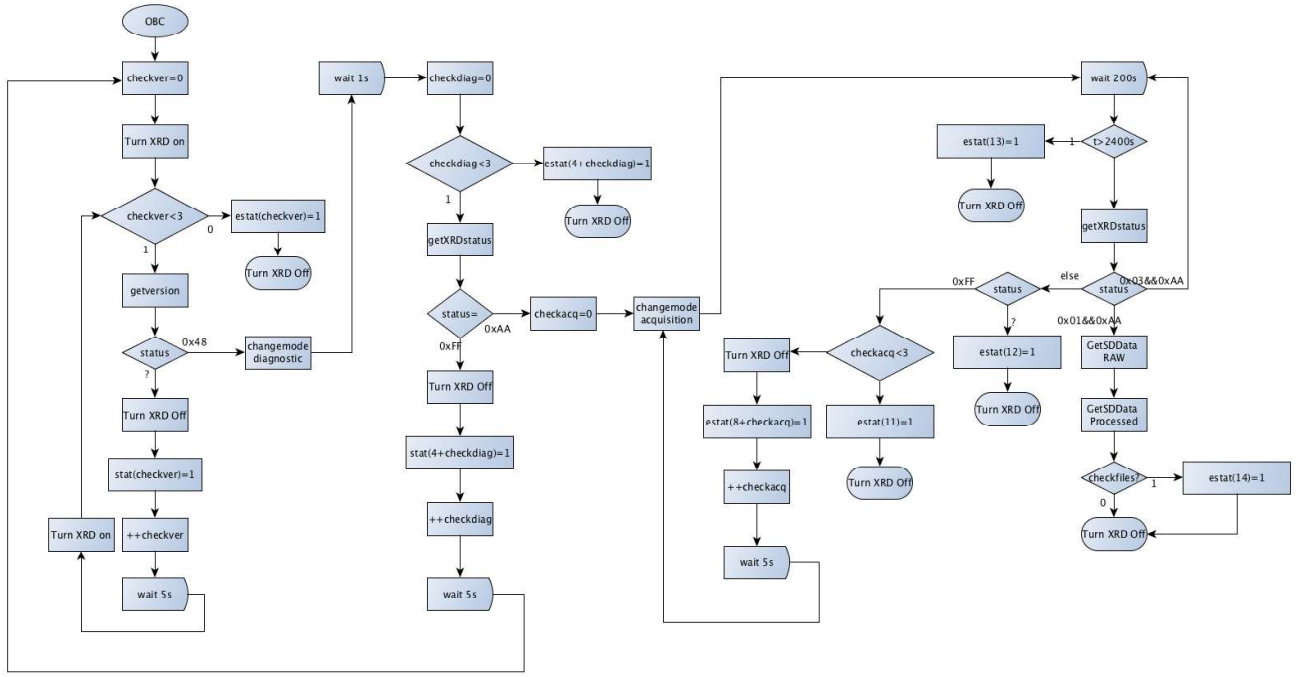


Fig. 3. Simplified flow diagram of the operation.

the board. Both the anodes and the cathodes are AC coupled to the RENA ASIC through coupling capacitors.

A single commercially available RENA-3b ASIC performs the initial readout of all anode and cathode strips (see Figure 2). RENA is a low-noise, 36-channel, self-trigger, self-resetting charge sensitive amplifier/shaper integrated circuit [12]. While it has never been tested in space, its low power consumption of <6 mW per channel and use of sub-micron CMOS process for fabrication are well suited for small satellite applications.

An MSP 430 microcontroller configures, controls and reads the analog outputs of the RENA chip. Since each channel can be individually configured for polarity, threshold, gain and shaping time, a single chip can read both anode and cathode strips. Once configured, signals exceeding the thresholds trigger the system. RENA sends the list of triggered channels to the MSP 430, and then the MSP 430 sequentially reads the analog outputs of triggered channels waiting at the peak & hold circuitry. The analog outputs are read directly at the ADC of the MSP 430 with a resolution of 12 bits.

The on-board computer (OBC) of the BeEagleSat can turn on and off the entire system. RENA requires 4 reference voltages to operate, 1.5 V, 2 V, 2.5 V, 3.5 V and also 5 V for power. MSP 430 can control the operation of the HV generator, it is turned on only during data acquisition. We are using UltraVolt US series HV supply to provide -250 V to cathodes. This HV supply provide low ripple and performed

well in TVAC tests [8].

The final XRD (Figure 2) board has been designed and produced as 6 layer PCB using ROGERS material. To protect the optically sensitive CdZnTe crystal from sunlight and any other stray light, the side of the PCB that the crystal is attached to is covered with a 1 mm thick aluminum enclosure preventing optical light but allowing most of the radiation above 20 keV. The cover is at ground potential reducing noise due to electromagnetic interference.

B. Software and Control

The communication with the OBC takes place with UART protocol. The system is designed to be turned on and off by the OBC via a switch at the input boost. The simplified flow diagram is given in Figure 3.

XRD can be driven into 3 operation modes by the commands from the OBC: "IDLE/SAFE MODE", "DIAGNOSTIC MODE", and "DATA ACQUISITION MODE". Before OBC releases the command to drive XRD to one of these modes, it checks if the MSP 430 is functional through the UART connection. This check is performed up to 3 times. In the IDLE/SAFE MODE, the HV is turned off and RENA is idle, all channels are turned off to save power. The DIAGNOSTIC mode only checks whether RENA receives configuration correctly by reading the threshold voltage of RENA channel 0, which can be set through the configuration. If diagnostic mode fails, the XRD is turned off, and this test repeats up to 3 times before shutting XRD off completely.

The main mode of operation is the "DATA ACQUISITION MODE". In this mode, RENA takes a pre-determined amount of data (adjustable, default 100,000 hits), or stops at timeout (default 2000 s). The raw data are written to the SD card for every 5 hits due to limitations of the MSP 430 RAM.

The raw data consist of anode and cathode strip identifiers that are hit for each trigger, and the signal on each strip. After data acquisition is finished, the raw data are converted into spectra. For diagnostic purposes on the ground, some of the raw data are also saved for telemetry. Each time XRD goes into DATA ACQUISITION mode, 2 files are created in the SD card: 1. Raw Data (2 kb), 2. Processed Data (singles spectrum, doubles spectrum, anode-only spectrum, light curve and logs reporting the results of diagnostics, rates of different types of events, total 17 kb). Once all the files are created, XRD waits for OBC commands to release data. Once transfer finishes, OBC turns the XRD off until the next acquisition.

C. Current Status of BeEagleSat and the XRD

During the ground tests of the XRD, we encountered problems regarding noise. To mitigate noise related problems we increased the trigger threshold and shut down most of the readout channels. Since the original design had seven non-rechargeable batteries in the BOTTOM side of the PCB [7], we placed all analog and digital electronics in a small area on the TOP side close to the noise sensitive RENA ASIC. We suspect this high concentration of circuit elements and/or poor grounding scheme in the PCB design caused the noise problem.

The XRD can only be turned on with commands from the ground station, and we have not implemented any mode for self-operation. The XRD on BeEagleSat could not be tested since its operation required an uplink command which could not be issued due to BeEagleSat receiver antenna problem. The BeEagleSat is about to complete its orbital lifetime and expected to burn down the atmosphere by the end of April 2019. Therefore the space qualification of the XRD system cannot be completed.

III. IMPROVED XRD, iXRD

With the experience we obtained from the XRD, we have started the design and development of the "Improved XRD, iXRD". The improvement is underway in two aspects of the design, eliminating the high noise observed in XRD, and improving the scientific return by increasing the size of the active area and limiting the field of view with a collimator.

A. The Detector in XRD

One of the improvements in the iXRD is using a larger volume crystal. We are planning to use a 25.4 x 25.4 x 5 mm³ COTS pixellated detector (see Fig. 4) produced by eV Products (currently Kromek). The crystal has 256 pixels with 1.6 mm pitch. It is attached to a PCB which has standard Samtec connectors. The same detectors are used in gamma

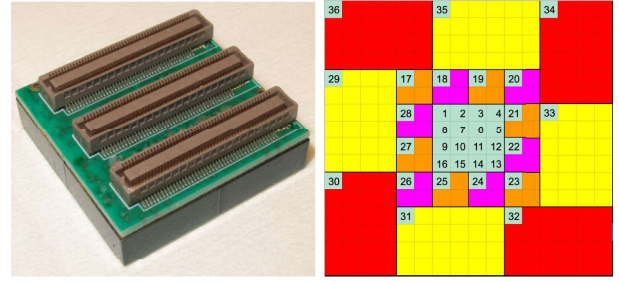


Fig. 4. Left: Picture of the crystal and connectors that will be used in iXRD. Right: Pixel map to cover 256 pixels with 36 readout channels

cameras operating in our labs and providing very good energy resolution (6 keV @ 122 keV for a single pixel). Not only the area is almost three times larger than the crystal in XRD, but the larger depth would also provide larger stopping power important for high energy photons (> 100 keV). While pixel design would provide better resolution compared to strips, we need to merge several pixels in the detector because RENA only has 36 readout channels. The pixel map is given in Fig. 4, right panel. This map indicates that different regions in the crystal will have different energy resolution, the middle part with 16 pixels will have the best resolution.

No change in readout ASIC is anticipated from the current design of the XRD. Any change in readout ASIC would require a complete redesign of the electrical power system as well as writing a control software from scratch. We emphasize that while the control software will stay the same, there may be significant changes in the storage and telemetry of data. How this data volume will be utilized will be decided based on the science mission and the details of the communications equipment and bandwidth.

While the ASIC will stay as RENA 3b, and the EPS and control (MSP 430) components are the same, there will be a significant change in the PCB design to mitigate noise problems that we encountered in the XRD. The iXRD will have a "motherboard - daughterboard" structure (see Fig. 5). The daughterboard will carry the crystal, coupling capacitors and the RENA without any other active components. All the EPS and control related components will be in the motherboard. Both boards will have 8 layers with plenty of ground layers.

B. Collimator

Hard X-ray collimators are often manufactured using lead or tungsten due to the high density and high atomic number of these materials. While machining lead is easier than machining tungsten, mechanical properties of tungsten are more suitable for space applications. The CXBN-I collimator was produced using a graded-Z (lead-tin-copper) combination to minimize background from atomic emission occurring in the collimator. CXBN-II used an additive manufactured tungsten collimator with square holes. In Turkey, we were not able to find a company that can do 3D printing with

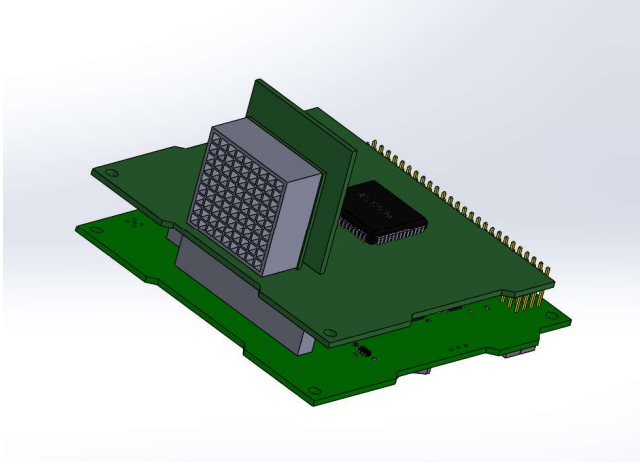


Fig. 5. Left: Technical drawing of a possible geometry of the iXRD with the collimator. Collimator size, pixel size and placement have not been determined yet. The system consists of a motherboard at the bottom and the daughterboard at top.

tungsten material but we have found a company that can machine tungsten. A possible configuration is shown in Fig. 5.

The pixel size and the length of the collimator depend on the science prospects of iXRD. The three science prospects currently under study are:

- Measuring cosmic X-ray background between 20 and 60 keV, essentially improving the results obtained with CXBN-I and CXBN-II.
- Getting hard X-ray spectrum of bright solar flares.
- Staring at chosen bright hard X-rays sources.

To measure cosmic X-ray background, a relatively large 30–40 degrees full width half maximum (FWHM) field of view is enough and the attitude control of the satellite is not critical. On the other hand, staring at bright hard X-ray sources requires a few degrees FWHM, three-axis control with a few degrees attitude control and even better attitude knowledge. Observing the Sun brings in other thermal constraints. The science prospects and details of the collimator parameter will be discussed in an upcoming paper when the detailed attitude control and determination properties of the host satellite is determined.

C. Current status of the iXRD

The iXRD development consists of 7 steps:

- Redesigning the motherboard to carry EPS and control circuitry
- Designing a daughterboard with the crystal and RENA
- Designing a collimator based on science mission and manufacturing capability
- Tweaking software to accommodate larger data volume
- Conducting simulations for further collimator optimization and to determine background in orbit
- TVAC and vibration tests
- Satellite integration

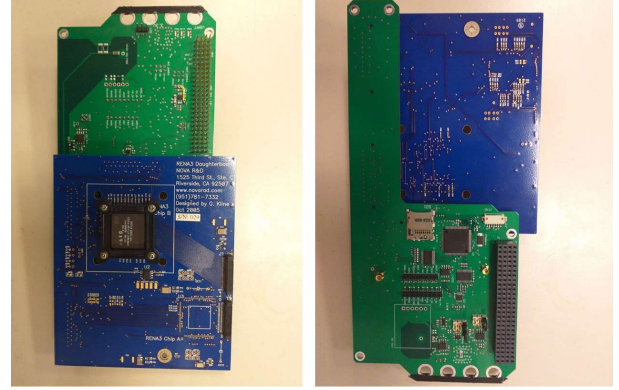


Fig. 6. Pictures of the desktop motherboard and the RENA test daughterboard during electrical and software tests.

Currently, we have completed the redesign of the motherboard, produced a desktop model and conducting electrical and noise tests with the desktop model (see Fig. 6). The desktop model has been designed to accommodate the daughter board of the commercial RENA test board to complete software tests as well. To access test points easily, the daughterboard over the desktop model is shifted to one side. In the actual design, they will be on top of each other and it will fit into 1U.

The design of the daughterboard is underway, the final design requires knowledge of the placement of the collimator. Possible collimator parameters have been determined and a company that could produce the collimator has been determined. As soon as the science mission is finalized both designs can be finalized and manufacturing can begin.

IV. CONCLUSIONS AND FUTURE PROSPECTS

An improved version of the XRD on BeEagleSat has been designed and currently in the production phase. The major improvements compared to the XRD are the larger volume crystal with almost three times the area, a collimator to limit the field of view for focused scientific return, and a motherboard-daughterboard design to reduce the noise. Currently we are testing the motherboard design, working on the daughterboard design and manufacturing the collimator.

The iXRD is expected to be tested in LEO onboard a 3U CubeSat Sharjah-Sat-1 [Sharjah-Sat-1, status to be presented in RAST2019] by the end of 2020. Sharjah-Sat-1 is developed by ITU-SSDTL and University of Sharjah (UoS). Sharjah-Sat-1 is expected to have an S-band antenna significantly improving the science prospects of the iXRD. The development of iXRD is supported both by ITU-SSDTL and UoS.

ACKNOWLEDGMENT

The iXRD development is also supported by UoS. Emrah Kalemci also thanks Onur Cengiz for technical drawing in Fig. 5.

REFERENCES

- [1] E. Kalemci, "Summary of the past, present and future of the X-ray astronomy", *Eur. Phys. J. Plus*, vol. 133, p. 407, Oct. 2008.
- [2] E. L. Shkolnik, "On the verge of an astronomy Cubesat revolution", *Nature Astronomy*, vol. 2., pp. 374–378, May 2018.
- [3] S. D. Barthelmy, L. M. Barbier, J. R. Cummings, et al., "The Burst Alert Telescope (BAT) on the SWIFT Midex Mission", *Space Sciences Review*, vol. 120, pp. 143–164, 2005.
- [4] F. A. Harrison et. al., "The Nuclear Spectroscopic Telescope Array (NuSTAR) High-energy X-Ray Mission", *ApJ*, vol. 770 p. 103, 2013.
- [5] L. M. Simms, J. G. Jernigan, B. K. Malphrus, et al., "CXBN: a blueprint for an improved measurement of the cosmological x-ray background", in: *Hard X-Ray, Gamma-Ray, and Neutron Detector Physics XIV*, Vol. 8507 of *Proc. SPIE*, p. 850719, 2012.
- [6] J. Healea, B. Malphrus, S. Mckneil, et al., "The Cosmic X-ray Background NanoSat-2 (CXBN-2): An improved measurement of the diffuse X-ray background," 12th Annual CubeSat Developers Workshop, Cal Poly, San Luis Obispo, CA, USA, April 22–24, 2015
- [7] E. Kalemci, E. Umit, R. Aslan, "X-ray detector on 2U cubesat BeEagleSAT of QB50", in: *Proceedings of 6th International Conference on Recent Advances in Space Technologies*, 12–14 June 2013, Istanbul, Turkey, IEEE, pp. 899–902. 2013.
- [8] A. R. Aslan, E. Kalemci, E. Umit, et al., "Development and in orbit testing of an x ray detector within a 2U cubesat", in *Proceedings of the 65th International Astronautical Congress*, Toronto, Canada, 2014.
- [9] A. Zappettini, M. Zha, L. Marchini, et al., "Boron Oxide Encapsulated Vertical Bridgman Grown CdZnTe Crystals as X-Ray Detector Material", *IEEE Transactions on Nuclear Science* vol. 56, pp. 1743–1746, 2009.
- [10] E. Kalemci, J. L. Matteson, R. T. Skelton, P. L. Hink, K. R. Slavis, "Model calculations of the response of CZT strip detectors", in: R. B. James, R. C. Schirato (Eds.), *Hard X-Ray, Gamma-Ray, and Neutron Detector Physics*, Vol. 3768 of *Proc. SPIE*, pp. 360–373, 1999.
- [11] E. Kalemci, J. L. Matteson, "Investigation of charge sharing among electrode strips for a CdZnTe detector", *Nuclear Instruments and Methods in Physics Research A* 478 pp. 527–537, 2002.
- [12] T. O. Tumer, V. B. Cajipe, M. Clajus, S. Hayakawa, A. Volkovskii, "Performance of RENA-3 IC with position-sensitive solid-state detectors", in: *Hard X-Ray, Gamma-Ray, and Neutron Detector Physics X*, Vol. 7079 of *Proc. SPIE*, p. 70791F, 2008.